J Mater Sci: Mater Med (2008) 19:3057–3062
DOI 10.1007/s10856-008-3444-z

Study on antibacterial mechanism of copper-bearing austenitic antibacterial stainless steel by atomic force microscopy

Li Nan · Yongqian Liu · Manqi Lü · Ke Yang

Received: 29 January 2008 / Accepted: 19 March 2008 / Published online: 5 April 2008

Abstract A study was made on the antibacterial mechanism of copper-bearing austenitic antibacterial stainless steel by a series of methods such as atomic force microscopy (AFM) observation, force–distance curves and inductively coupled plasma mass spectrometer test. It was observed by AFM that the structure of the outer cell membrane responsible for the cell permeability was substantially changed for the bacteria after contacting with the antibacterial stainless steel, showing that cell walls were seriously damaged and a lot of contents in the cells leaked. It was also found that the adhesion force of bacteria to antibacterial stainless steel was considerably greater than that to the contrast steel, indicating that the electrostatic forces by Cu^{2+} being an important factor for killing bacteria.

1 Introduction

Escherichia coli (*E. coli*) is a kind of Gram-negative bacteria with a cell membrane and wall model as shown in Fig. 1 [1–3]. The cell wall is positioned outside the cell membrane and directly contacts the environment. This structure consists of an outer lipopolysaccharide (LPS) membrane overlying a gel-like periplasm and a thin peptidoglycan inner layer [4, 5]. Approximately 75% of the outer membrane of the cell wall is LPS while the remaining 25% is composed of membrane proteins that may be compactly folded and form dense structures, which probably represent the rigid regions of the cell wall [6, 7]. The outer cell wall may also contain a variety of external structures, such as fibrils, fimbriae, pili and flagella [8, 9]. The combination of all of these structures determines the physicochemical properties of the cell surface for a particular bacterial strain. Loss or damages of LPS molecules would lead to an increase in the permeability of the cell wall.

At present, though some researches have been made on the antibacterial mechanism [10, 11], few results have been acquired to reveal the process of inhibiting and killing bacteria. As to the antibacterial mechanism of metal ions, some possible mechanisms have been put forward. For instance, bacteria are killed by metal ions through absorption in the electric field, or a catalysis process, or damage of the enzymatic system that affects the normal metabolism, and so on [12].

Recently, the force measurements by atomic force microscopy (AFM) on the cell–solid and cell–cell interactions using the functionalized probes have been shown to be a promising approach to study the initial bacteria attachment [13]. The bacteria are directly attached to the end of the cantilever to form a modified tip, termed as a cell probe. Cell probes have been used to quantify the interactions between the bacteria and various inanimate surfaces [14]. As bacteria move toward a solid surface, the initial interaction between a bacterial cell and the surface is governed by the long and medium range forces, primarily van der Waals and electrostatic forces [15, 16]. These forces depend on the physicochemical properties of the substratum and the bacterial surface, such as hydrophobicity [17], free energy [18] and surface charge [17].

L. Nan · Y. Liu · M. Lü · K. Yang (✉)
Institute of Metal Research, Chinese Academy of Sciences, Shenyang 110016, China
e-mail: lnan@imr.ac.cn

L. Nan · Y. Liu
Graduate School of Chinese Academy of Sciences, Beijing 100049, China

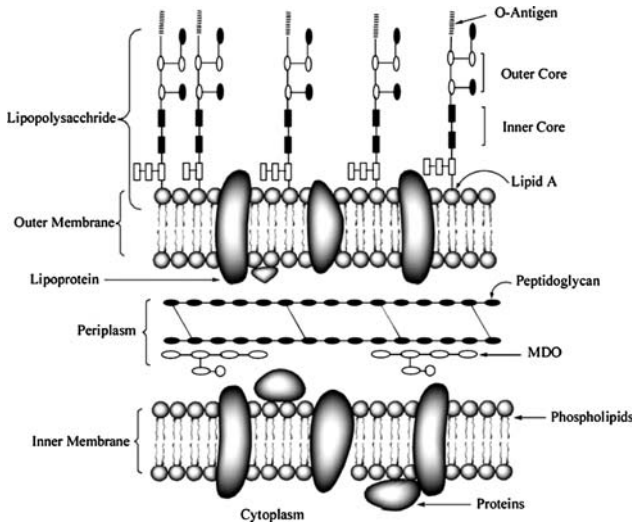

Fig. 1 Schematic molecular representation of *E. coli* envelop [1–3]. The envelop of Gram-positive bacterium consists of the outer membrane, the inner membrane and the peptidoglycan layer. MDO is the membrane-derived oligosaccharides

Based on the previous research, this work conducted a preliminary investigation on the antibacterial mechanism of the copper-bearing austenitic antibacterial stainless steel against *E. coli* by using some special research methods. The information that was obtained may lead to a better understanding of the antibacterial mechanism of such novel steel.

2 Materials and experiments

2.1 Bacteria

The Gram-negative bacteria used in this study, Escherichia coli ATCC 25922 (*E. coli*), were obtained from a preserving center for bacteria in China. The bacteria were cultured in a Luria-Bertani (LB) medium (g/l): peptone 10.0, NaCl 5.0, beef extract 5.0. The pH was adjusted to 7.0 $\sim$ 7.2 using 0.5 M NaOH solution.

2.2 Sample preparation

In this study, the antibacterial material was a copper-bearing austenitic antibacterial stainless steel (0Cr18Ni9-3.8 wt pct Cu), and the material for comparison was the corresponding austenitic stainless steel (0Cr18Ni9), which were developed by Institute of Metal Research, Chinese Academy of Sciences, Shenyang, China. Experimental samples were cut into slices (10 mm $\times$ 10 mm $\times$ 1 mm). The samples were mechanically polished with wet SiC papers until 1200 grit and then finely polished with 1.5 μm Al_2O_3 powders paste for optical observation.

2.3 AFM analysis

AFM imaging was performed on a Nanoscope (R)III Bioscope AFM (Digital Instruments, Veeco Metrology Group, CA, USA). The relative humidity was 50–60% and no capillary forces were observed during operation. The nanoprobe cantilevers of silicon nitride (Si_3N_4) had a spring constant of $K = 0.12$ N/m (DI). The radius of curvature of AFM tip was approximately 5 nm. The Digital Nanoscope software (version 5.12) was used to analyze the topography of the cell surface. All the AFM images were only treated with the flatten command.

The topographic images of the surface as well as the force–distance over the sample surface were recorded. In the force vs. distance measurements, the tip/substrate approach speed in *z*-direction was varied from 0.1 μm/s to 100 μm/s. Each map of the sample surface consisted of 512 $\times$ 512 grid points.

The culturing solution (0.1 M NaCl) containing the bacteria was diluted to 10^8 cfu/ml, and then 18 μl of bacterial solution was added onto the surface of samples for the observations on AFM at separate times of 3 h, 9 h and 24 h cultures.

2.4 Analysis of force curves

It has been found that the physiological properties of bacteria, namely the bacterial surface charges and hydrophobicity, also have influence on the bacteria interaction. The cell–cell interactions showed that there are strong electrostatic repulsion forces between bacterial cells. The cell probe of AFM has provided some useful insights into the interactions of bacterial cells on metal surfaces.

Figure 2 illustrates a typical force–distance curve between the Si_3N_4 tip and the cells surface. As the sample extends upward approaching the tip from A to B shown in Fig. 2, the tip is pulled down by the attractive force and jump-to-contact with the surface at B. As the sample

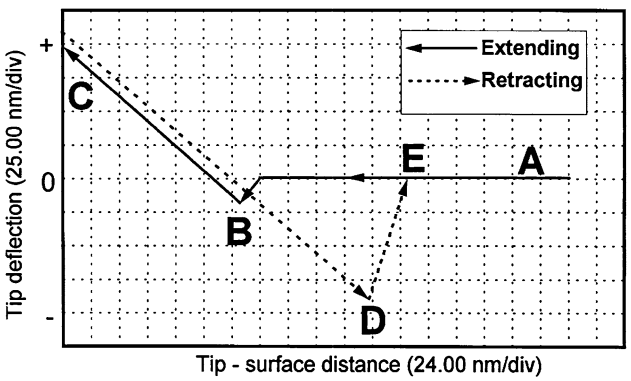

Fig. 2 A typical force–distance curve between the AFM tip and bacterial surface [19]

continues to extend, the cantilever bends upward as the tip presses onto the surface. When the tip reaches position C, the sample retracts from the tip and the cantilever relaxes. As the sample continues to retract, the cantilever begins to bend downward (CD) due to the adhesion force, until reaching the break point (D) at which the cantilever rebounds sharply upward to E. The adhesion force between the tip and the surface can be calculated from the deflection distance of cantilever and the cantilever spring constant, as follows:

$$F = k \times \Delta L$$

where F is the force (nN), k is the spring constant of cantilever, which was equal to 0.12 N/m in this study, and ΔL is the deflection distance (nm), which is the vertical distance between points D and A in Fig. 2. The reference zero of deflection is point A, when the tip is far away from the surface. A negative deflection corresponds to the attractive force whereas a positive deflection to the repulsive force.

The force–distance curve also provides additional information related to the elasticity of the sample surface. The cantilever deflection increases as the tip continues to press into the sample after contact, as represented by the repulsive section of the force curve BC in Fig. 2. The slope of the BC section of the force curve represents the surface elasticity [19].

Physicochemical characterization and adhesion tests of the bacteria were performed on the cells in stationary growth phase. The bacteria were harvested by a centrifugation (10 min, 7,000 × g, 4°C), and washed twice and resuspended in 0.1 M NaCl solution. Then, the suspension was diluted to a cell concentration of 1×10^8 cfu/ml. Using a modified bacterial tip, the attraction and repulsion forces, in the nano-Newton range, between the bacterial cell and the metal surface in aqueous media were quantified.

2.5 Analysis of K^+ and Cu^{2+} in the supernatant

An Inductively Coupled Plasma Mass Spectrometer (ICP-MS), OPTIMA3000 from USA, was used in this study to determine the amount of K^+ and Cu^{2+}. ICP-MS is a method for raped and sensitive determination of all the considered elements, which is sufficiently sensitive to detect 1 ng/l of elements [20, 21]. The concentrations of K^+ and Cu^{2+} in the supernatant obtained from the above experiments were analyzed by ICP-MS. The initial concentration of bacteria was 10^8 cfu/ml.

3 Results and discussion

3.1 Imaging of cells

The morphology changes of *E. coli* acted with the antibacterial stainless steel and the contrast stainless steel for different time were observed under AFM, as shown in Fig. 3. A normal *E. coli* should look short-stick and edge-trim, and its cell wall is compact and intact. After acting with the antibacterial stainless steel for 3 h, it can be seen from Fig. 3b that the cell walls of *E. coli* were not changed too much. When the action time was 9 h, Fig. 3c shows that the outer membrane collapsed while the inner part of the cell still remained intact. After acting with the antibacterial steel for 24 h, the whole cells turned thin and shriveled, as shown in Fig. 3d. It is postulated that the debris originates from the bacterial periplasm. Cu^{2+} should at first bind to the negatively charged LPS of GNB to enable its initial penetration into the bacterial outer membrane and hence, releasing the periplasmic material. Also, leakage of the fluid was found to be at the poles of the bacteria. Thus, it is possible that the apical ends were where the bacteria were targeted first, or where the damage was first concentrated. This is logical since the domains of cardiolipin, the negatively charged phospholipids, should reside at the apical ends of inner membrane of *E.coli*, other than the septal regions. Therefore, probably the peptides were concentrated at the apical ends, which initiated the cell leakage. While acting with the contrast stainless steel for 24 h, the morphology of *E. coli* was nearly not changed, as shown in Fig. 3a.

The above result indicates that, after acting with the antibacterial stainless steel, the cell membrane or cell wall of bacteria was destroyed, permeability of the cell was increased and the inner contents were much leaked, thus leading to death of bacteria.

3.2 Analysis of force curves

The initial bacterial attachment is formed through a reversible adsorption process, which is governed by electrostatic attraction and physical forces, e.g., van der Waals force and hydrophobic interactions [13, 22], instead of a chemisorption. The adhesion forces are dependent on the physicochemical property of the substrate and the surface feature of bacteria, e.g., hydrophobicity and surface charge. In general, some of the adsorbed cells can colonize and form structures which may permanently hold the cells to the surface to form a biofilm. The initial bacterial attachment is a crucial step in the process of biofilm development [17].

The slope of a force–distance curve after the initial tip contact with the sample represents the elasticity of the cell surface. From Fig. 4, the adhesion forces of cell–cell, cell-antibacterial stainless steel and cell-contrast steel were determined to be 0.88 nN, 1.13 nN and 0.94 nN, respectively. This shows that the adhesion force on antibacterial steel is considerably higher than that on bacteria and contrast steel. It seems to suggest that the accumulation of

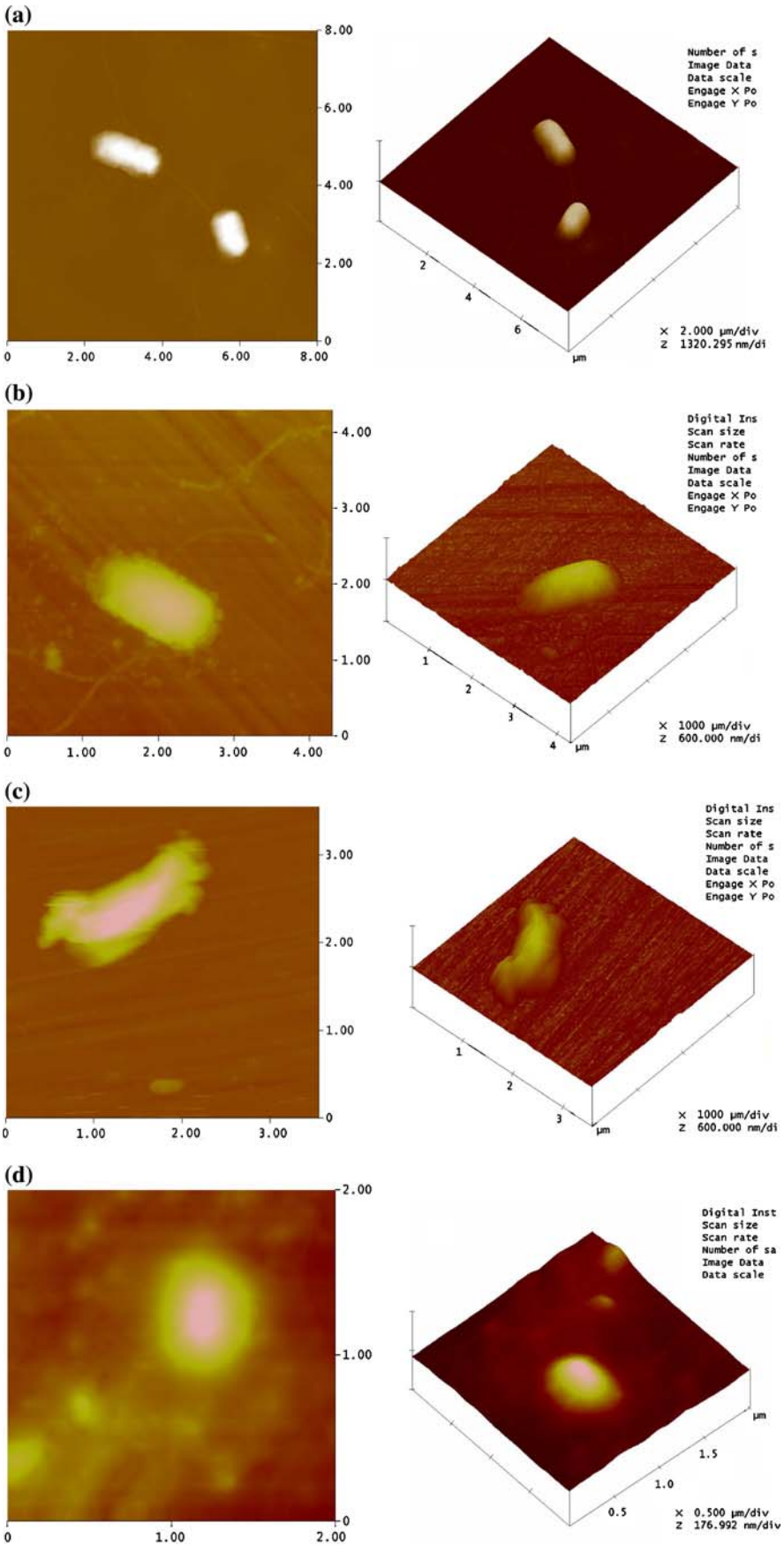

Fig. 3 Morphologies of bacterial cells for different action time, (**a**) with the contrast steel from beginning to 24 h (2D,3D); (**b**) with the antibacterial stainless steel for 3 h (2D,3D); (**c**) with the antibacterial stainless steel for 9 h (2D,3D); (**d**) with the antibacterial stainless steel for 24 h (2D,3D)

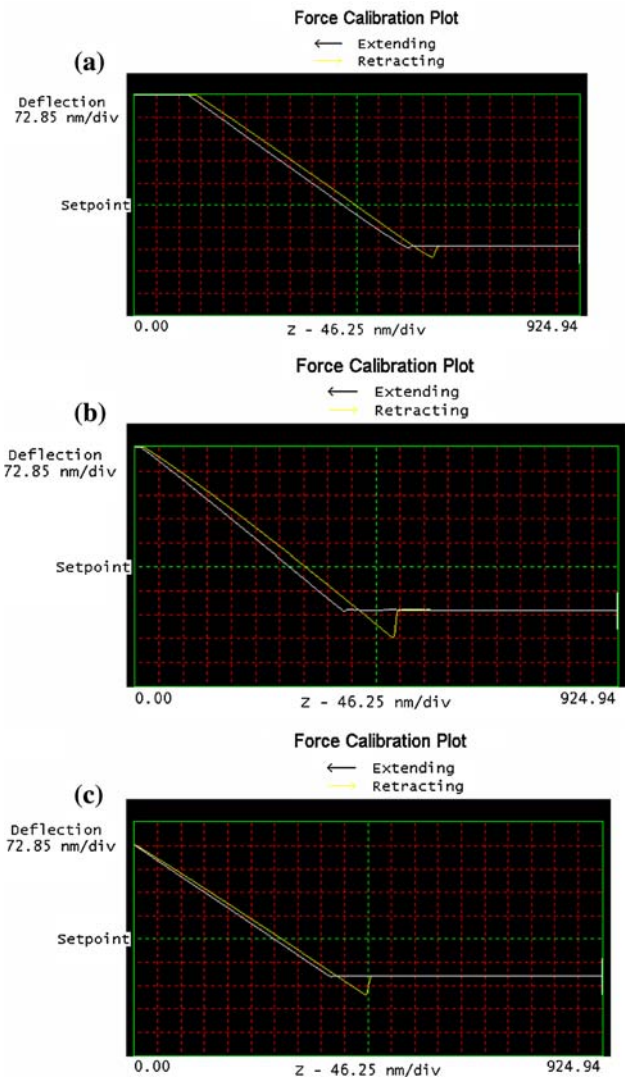

Fig. 4 Bacterial adhesion forces on the different surfaces, (**a**) adhesion force between bacteria; (**b**) adhesion force between bacteria and the antibacterial stainless steel; (**c**) adhesion force between bacteria and the contrast steel

sticky EPS on cell-antibacterial steel interface would enhance the aggregation of bacterial cells, leading to the formation of a spreading biofilm. The cell–cell force curve indicates that once a layer of bacteria was adsorbed to the metal surface, it would become difficult to adsorb other bacteria to the former bacterial layer. Furthermore, cell–metal force curve shows that bacteria were much more adsorbed to the antibacterial stainless steel than the contrast steel.

Therefore, a conclusion may be drawn that the bacterial adhesion forces to metals should be influenced by both the electrostatic force and the hydrophobicity of metal surface. As to the reports [13, 22], the strength of adhesion forces depends on the electrostatic forces. Changes of the adhesion forces on different materials indicate that *E.coli* is susceptible to antibacterial steel, making the contact easier on antibacterial steel than on contrast steel, promoting the action between copper ions and bacteria, causing bacterial metabolic disturbance, and leading to death of bacteria, which are supported by some reports [12]. In addition, Rotsch and Radmacher [23] found in an AFM study that the interaction forces between the tip and a charged surface were affected by the ionic strength, which may also affect the elasticity of the cell surface. However this issue is beyond the scope of current study and further investigation is needed to warrant it.

3.3 Concentration of K^+ and Cu^{2+}

It is well known that K^+ plays important role in maintaining bacterial energy metabolism and cellular normal osmotic pressure. When the K^+ from the cell was leaked, the internal–external osmotic pressure of the cells would be changed and metabolism would be disordered, even leading to death of bacteria [24].

It can be seen from Fig. 5a that the concentration of K^+ in the bacterial solution after the action between bacteria and the antibacterial stainless steel was much higher than that of the action between bacteria and the contrast steel.

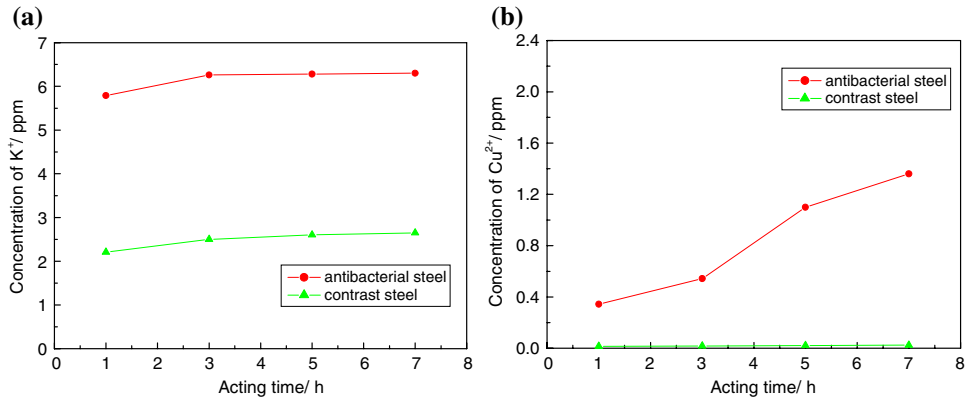

Fig. 5 Time curves of different metal ions in the supernatant liquid (**a**) K^+, (**b**) Cu^{2+}

Through testing at the beginning, the initial concentration of K^+ is 1.37 mg/l in the bacterial solution. When the action time was 1 h, the concentration of K^+ increased to 2.58 mg/l and 1.39 mg/l in the solutions that were contacted by the antibacterial stainless steel and the contrast steel, respectively. With the action time prolonged, the concentration of K^+ was gradually raised. When the time approached to 7 h, the concentration of K^+ in the two solutions increased to 5.79 mg/l and 2.65 mg/l, respectively. The results indicate that through the action of the antibacterial stainless steel to the bacteria, the K^+ in the cells was much leaked to outside, which proved that the internal–external osmotic pressure of the cells was changed and the metabolism of energy was disordered by this action.

In addition, the concentration of Cu^{2+} in the supernatant was increasing with the time of action between antibacterial stainless steel and bacteria, as shown in Fig. 5b. It indicated that when the antibacterial stainless steel was contacted with bacteria for a certain period time, the copper ions could be dissolved from the ε-Cu phases on the surface of the steel, killing the bacteria on the surface of steel. With time prolonged, the quantity of Cu^{2+} increased, and then more cells wall and cell membrane were destroyed, which should be one of the main reasons leading to death of bacteria finally, similar to the antibacterial mechanism of La^{3+} on GNB [25].

4 Conclusions

The dissolved copper ions play the dominant role for the antibacterial effect of antibacterial stainless steels acted with *E. coli*, which leads to the collapse of some LPS patches of the cell surface, and consequently alters the permeability and functionality of the outer cell membrane. These provide the structural basis for the antibacterial effects of Cu^{2+} on the microorganism. High resolution AFM allows the direct visualization of the change of cell membrane structure at the nanoscopic level as well as the measurement of the interaction force between bacteria and the metal substrate. ICP-MS is an effective tool to support the assertion about the antibacterial effect of Cu^{2+} from the steel. Further work needs to be done to investigate the interaction of with inner membrane and cytoplasm.

Acknowledgement This work was financially supported by a fund from National Natural Science Foundation (No. 50671101).

References

1. L. Chen, W.G. Coleman Jr., J. Bacteriol. **175**(9), 2534–2540 (1993)
2. M.T. Silva, J.C.D.F. Sousa, J. Bacteriol. **113**(2), 953–962 (1973)
3. C.R.H. Raetz, Anuu. Rev. Biochem. 59, 129–170 (1990)
4. X. Yao, M.H. Jericho, D.F. Pink, T.J. Beveridfge, J. Bacteriol. **181**, 6865 (1999)
5. X. Yao, J. Walter, S. Burke, S. Stewart, M.H. Jericho, D. Pink, R. Hunter, T.J. Beveridge, Colloids Surf. B Biointerfaces **23**, 213 (2002)
6. N.A. Amro, L.P. Kotra, K. Wadu-Mesthrige, A. Bulychev, S. Mobashery, G.Y. Liu, Langmuir **16**, 2789 (2000)
7. P. Schaer-Zammaretti, J. Ubbink, Ultramicroscopy **97**, 199 (2003)
8. Y.F. Dufrene, Ch.J.P. Boonaert, H.C. van der Mei, H.J. Busscher, P.G. Rouxhet, Ultramicroscopy **86**, 113 (2001)
9. V. Vadillo-Rodriguez, H.J. Busscher, W. Norde, J. de Vries, H.C. van der Mei, Langmuir **19**, 2372 (2003)
10. C.C. Trapalis, M. Kokkoris, G. Perdikakis, G. Kordas, J. Sol-Gel Sci. Technol. **26**, 1213–1218 (2003)
11. Z.G. Dan, H.W. Ni, B.F. Xu, J. Xiong, P.Y. Xiong, Thin Solid Films **492**, 93–100 (2005)
12. L. Nan, W. Yang, Y. Liu, H. Xu, Y. Li, M. Lu, K. Yang, J. Mater. Sci. Tecnol. **24**, 197–201 (2008)
13. Y.F. Dufrêne, Curr. Opin. Microbiol. 6, 317–323 (2003)
14. Y. Ong, A. Razatos, G. Georgious, M.M. Sharma, Langmuir **15**, 2719–2725 (1999)
15. M. Fletcher, in *Bacterial Adhesion: Molecular and Ecological Diversity*, ed. by M. Fletcher (Wiley–Liss, New York, 1996), pp. 1–24
16. A. Razatos, Y. Ong, M.M. Sharma, G. Georgious, Proc. Natl. Acad. Sci.USA **95**, 11059–11064 (1998)
17. J.T. Gannon, V.B. Manilal, M. Alexander, Appl. Environ. Microbiol. **57**, 190–193 (1991)
18. H.J. Busscher, A.H. Weerkamp, H.C. van der Mei, A.W.J. van Pelt, H.P. De Jong, J. Arends, Appl. Environ. Microbiol. **48**, 980–983 (1984)
19. M. Radmacher, M. Fritz, H.G. Hansma, P.K. Hansma, Science **265**, 1577–1579 (1994)
20. P. Roth, E. Werner, I. Wender, P. Schramel, Appl. Radiat. Isot. **47**, 1055–1056 (1996)
21. M. Barbaro, B. Passariello, S. Quaresima, A. Cascillo, A. Marabini, Microchem. J. **51**, 312–318 (1995)
22. C.J. van Oss, R.J. Good, M.K. Chaudhury, J. Colloid. Interface Sci. **111**, 378–390 (1986)
23. C. Rotsch, M. Radmacher, Langmuir **13**, 2825–2832 (1997)
24. W.C. Yang, Master Dissertation, Chinese Academy of Sciences, vol 7, (2007), p. 51 (in Chinese)
25. L. Peng, L. Yi, L. Zhexue, Z. Juncheng, D. Jiaxin, P. Daiwen, S. Ping, Q. Songsheng, J. Inorganic. Biochem. **98**, 68–72 (2004)